

na powder (P172SB, Péchiney) with a specific area of $10.2 \text{ m}^2 \text{ g}^{-1}$, a refractive index of 1.70, and a mean diameter of $0.5 \mu\text{m}$. A dispersant (phosphoric ester) is also used to decrease the viscosity and to increase the stability of the suspension. The final mixture is prepared with 80 wt.-% (50 vol.-%) of alumina, dispersant (1.5 wt.-% with respect to alumina) and photoinitiator (5.56 wt.-% with respect to the monomer) mixed in a ball mill for 20 min at 350 rpm.

The scraper is based on a 10 mm long scalpel. It is moved at a speed of 1.2 mm s^{-1} , which corresponds to a shear rate varying from 60 to 24 s^{-1} , depending on the layer thickness (from 20 to $50 \mu\text{m}$, respectively).

The debinding step consists of several heating steps. First, the sample is heated to 120°C (degradation temperature of the polymer) at 60°C h^{-1} . A slower second temperature gradient of 6°C h^{-1} is applied up to 500°C and the temperature is maintained for 30 min. The quick heating of the sintering step is applied by increasing the temperature at 900°C h^{-1} to 1550°C . The object to be sintered is kept at this temperature for 5 h, and is then cooled to ambient temperature.

Received: January 27, 2003

Final version: February 25, 2003

- [1] H. Löwe, W. Ehrfeld, *Electrochim. Acta* **1999**, *44*, 3679.
- [2] J. Hruby, S. Griffiths, L. Domeier, A. Morales, D. Boehme, M. Bankert, W. Bonivert, J. Hachman, D. Skala, A. Ting, *Proc. SPIE—Int. Soc. Opt. Eng.* **1999**, *3874*, 32.
- [3] H. Yang, P. Deschatelets, S. Brittain, G. Whitesides, *Adv. Mater.* **2001**, *13*, 54.
- [4] J. F. Li, S. Sugimoto, S. Tanaka, M. Esashi, R. Watanabe, *J. Am. Ceram. Soc.* **2002**, *85*, 261.
- [5] R. Knitter, W. Bauer, D. Göhring, J. Hausselt, *Adv. Eng. Mater.* **2001**, *3*, 49.
- [6] L. Wang, F. Aldinger, *Adv. Eng. Mater.* **2000**, *2*, 110.
- [7] H. Becker, C. Gärtner, *Electrophoresis* **2000**, *21*, 12.
- [8] U. P. Schönholzer, R. Hummel, L. J. Gauckler, *Adv. Mater.* **2000**, *12*, 1261.
- [9] J. W. Halloran, *Br. Ceram. Trans. J.* **1999**, *98*, 299.
- [10] X. Jiang, C. Sun, X. Zhang, *ASME MEMS* **1999**, *1*, 67.
- [11] P. F. Jacobs, *Rapid Prototyping and Manufacturing: Fundamentals of Stereolithography*, The Society of Manufacturing Engineers, Dearborn, MI **1992**.
- [12] S. Monneret, C. Provin, H. Le Gall, in *8th IEEE Int. Conf. on Emerging Technologies and Factory Automation (ETFA'01)*, Vol. 2, IEEE, Piscataway, NJ **2001**, p. 299.
- [13] C. Provin, S. Monneret, *IEEE Trans. Electron. Packag. Manuf.* **2002**, *25*, 59.
- [14] S. Monneret, C. Provin, H. Le Gall, S. Corbel, *Microsyst. Technol.* **2002**, *8*, 368.
- [15] C. Hinczewski, S. Corbel, T. Chartier, *Rapid Prototyping J.* **1998**, *4*, 104.
- [16] M. L. Griffith, Ph.D. Thesis, University of Michigan, Ann Arbor, MI **1995**.
- [17] C. Provin, S. Monneret, H. Le Gall, H. Rigneault, P. F. Lenne, H. Giovannini, in *Microreaction Technology, Proc. 5th Int. Conf. Microreact. Technol.* (Eds: M. Matlosz, W. Ehrfeld, J. P. Baselt), Springer, Berlin **2001**, p. 103.

Detection of CO and O₂ Using Tin Oxide Nanowire Sensors**

By Andrei Kolmakov, Youxiang Zhang, Guosheng Cheng, and Martin Moskovits*

Solid-state gas sensors play a major role in semiconductor processing, medical diagnosis, environmental sensing, personal safety, and national security, with economic impact in

[*] Dr. M. Moskovits, Dr. A. Kolmakov, Y. Zhang, Dr. G. Cheng
Department of Chemistry and Biochemistry
University of California
Santa Barbara, CA 93106 (USA)
E-mail: mmoskovits@lsc.ucsb.edu

[**] We thank Prof. A. Heeger, Dr. D. Moses, and Dr. G. Wang for the loan of essential equipment and for many helpful discussions. We are grateful to Mr. E. Caine and Dr. J. P. Zhang for their help with lithography and HREM. This work made extensive use of the MRL Central Facilities at UCSB supported by the National Science Foundation under award No. DMR96-32716.

agriculture, medicine, and in the automotive and aerospace industries.^[1–3] Most sensors operate on the basis of the modification of the electrical properties of an active element, normally a metal oxide film, brought about by the adsorption of an analyte on the surface of the sensor. A current major goal in gas sensing is massive parallelism, wherein many sensors, each with its unique chemical properties, are operated together and their outputs processed simultaneously, perhaps using learning strategies like neural networks, so that the overall device operates “intelligently”, mimicking, for example, the complex operation of a mammalian nose and its corresponding brain function.^[4] This task implies the need for further miniaturization of the active elements with the simultaneous sensitivity increase to compensate for surface area loss. Here, conventional thin film technology faces its fundamental limits. Promising strategies for achieving the above goal of using many sensing elements restricted to a small volume will likely come out of nanoscience and technology and, specifically, out of a subset of technologies amenable to parallelism and array fabrication that do not sacrifice sensitivity and selectivity. This challenge necessitates several design features to be achieved simultaneously, including the development of new materials, innovation in structure and architecture, and the development of highly sensitive, responsive, and selective, yet ultra-small active elements arranged so as to minimize inter-element cross-talk.^[5,6]

The high surface-to-volume ratio of nanowires makes them natural contenders as new sensors. Nanowires synthesized by a number of techniques,^[7–9] and carbon nanotubes^[10–13] have recently been proposed for a number of sensor applications with encouraging preliminary results. However, the major challenges of producing quasi-one-dimensional nanostructures composed of well-established sensor materials like SnO₂, ZnO, and TiO₂,^[14,15] and the integration of individual nanowires^[16,17] or nanowire arrays with planar technologies remain.

In this report, we posit a new paradigm for producing nanowire sensor arrays with possibly thousands of addressable sensing elements that can each be individualized, either through the manipulation of their material composition or the manner in which they are functionalized. By using self-organized, highly ordered porous anodic alumina (PAO) templates, we can controllably manufacture arrays of parallel nanowires with pre-defined compositions,^[18–22] diameters, and lengths. In this communication, we illustrate this possibility vividly with the successful realization^[23] of a functional and sensitive SnO₂ single nanowire sensor synthesized by topotactically converting a tin nanowire sequentially to p-type SnO then to n-type SnO₂. We also demonstrate that the diameters of the SnO₂ nanowires we produce ($\approx 60 \text{ nm}$) are small enough for the adsorption of oxidizing or reducing gases on their surfaces to alter the bulk electronic structure of the entire nanowire, and not merely its surface region. In other words, we have produced what is, in essence, a conductance switch, the bulk conductivity of which is fully determined by its surface chemistry.

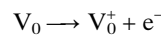
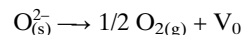
The fabrication of PAO membranes and subsequent nanowire growth inside the template's pores have been described previously.^[24–27] The process is summarized in Figure 1. Highly crystalline individual metallic β -Sn nanowires are grown by alternating current (AC) electrodeposition (80 V peak-to-peak, 200 Hz) in an electrolyte containing 0.05 M $\text{SnCl}_2 \cdot \text{H}_2\text{O}$ and removed from the PAO template either by etching of the alumina matrix (Fig. 1c) in NaOH (for X-ray diffraction (XRD) measurements), or by cracking the oxide and sonicating the nanowires loose, and then carefully oxidizing them by gradual annealing up to 825 K for a few hours in air. In-situ XRD analysis (Fig. 1e) performed on an assembly of nanowires shows the conversion of Sn initially to the metastable intermediate, tin suboxide, whose growth begins at ~ 470 K, simultaneously with a significant decrease in metallic tin (Fig. 1f). The intermediate p-type SnO phase is interesting

as a sensor material in its own right. On further heating, SnO begins to decrease at ~ 620 K with the simultaneous appearance of SnO_2 . At 825 K Sn is completely oxidized to tetragonal (rutile) tin oxide. The large domain size (>100 nm) deduced from the width of the XRD reflections and the morphological integrity of the nanowire after oxidation tested with scanning electron microscope (SEM) suggest that the conversion of the tin metal to tin oxide occurred topotactically (Fig. 1d).

Conductance measurements were performed on isolated individual nanowires outfitted with vapor-deposited Ti/Au micro-contacts. The stable currents measured result from the highly crystalline morphology of the nanowire giving rise to ohmic conductance as opposed to the more unstable percolating or hopping transport normally operating in cluster-based tin oxide sensor materials.

Current–voltage (I – V) measurements were carried out as a function of temperature and gas exposure in a gas cell equipped with microprobe contacts (Fig. 2a). The conductance and I – V characteristics of the nanowires depend critically on the temperature and the ambient gas partial pressure. In the absence of oxygen, the nanowire is a fairly good conductor (Fig. 2b), which is converted into an insulator in the presence of sufficient oxygen (Fig. 2c). This dramatic switch from conductor to insulator induced by the nature of the species adsorbed on the nanowire's surface is due to a change in the nanowire's bulk electronic properties, as immediately deducible from the striking change in carrier activation energy on exposure to oxygen (Fig. 2d).

The low resistance measured in the absence of an oxidant and its weak temperature dependence (Fig. 2b) are consistent with a highly doped semiconductor or a quasimetal. This behavior is likely due to the presence of easily ionizable oxygen vacancies, V_0 , in the n- SnO_2 that remain ionized over a wide temperature range.^[28,29] When annealed at high temperatures in an inert atmosphere the surface of the tin oxide loses many of the lattice $\text{O}_{(s)}^2$ and/or ionosorbed $\text{O}_{(s)}^-$ species and oxygen vacancies are formed in Equations 1 and 2 resulting in donor states which render the oxide an n-type semiconductor.



Here the sub-indices s and g refer to surface and gas, respectively; V_0 is a vacancy with two trapped electrons.

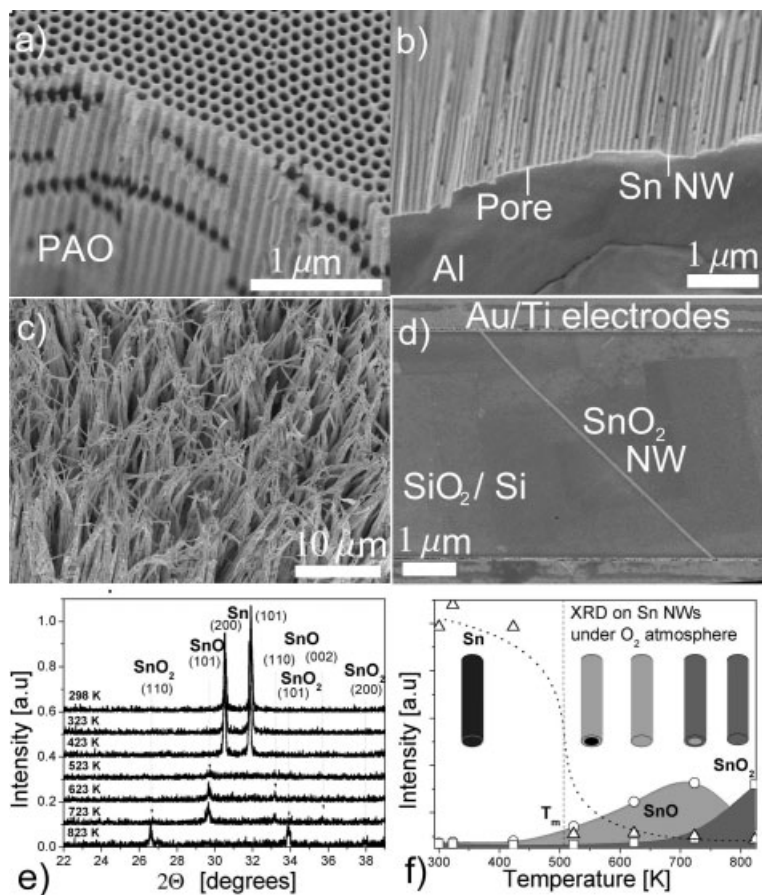


Fig. 1. Steps in the fabrication of SnO_2 nanowires arrays and the preparation of individual nanowires for conductance measurements. a) SEM image of highly regular porous anodic alumina template. b) SEM image of the PAO template cross-section with metal nanowires of desirable length, diameter, and composition grown inside the nanopores. c) Tin nanowires are released from their oxide matrix either by etching (shown in the figure) or by cracking the oxide host and sonicating the nanowires loose. d) To maintain morphology of the nanowire above the melting point of tin (505 K), a thin supporting oxide skin was grown on the surface of the tin nanowires by annealing the sample in air at 473 K for 2 h. After gradual thermal oxidation of an array of well-isolated nanowires, a single nanowire is extracted and deposited onto an oxidized Si substrate. Au/Ti electrodes are deposited either using electron beam (e-beam) lithography (shown in SEM image), or through a microwire-grid contact mask. e,f) Temperature-programmed XRD carried out on an ensemble of nanowires indicates that the oxidation process begins with pure Sn, forms an intermediate phase (romarchite, SnO) and eventually ends in the formation of SnO_2 (cassiterite) nanowires.

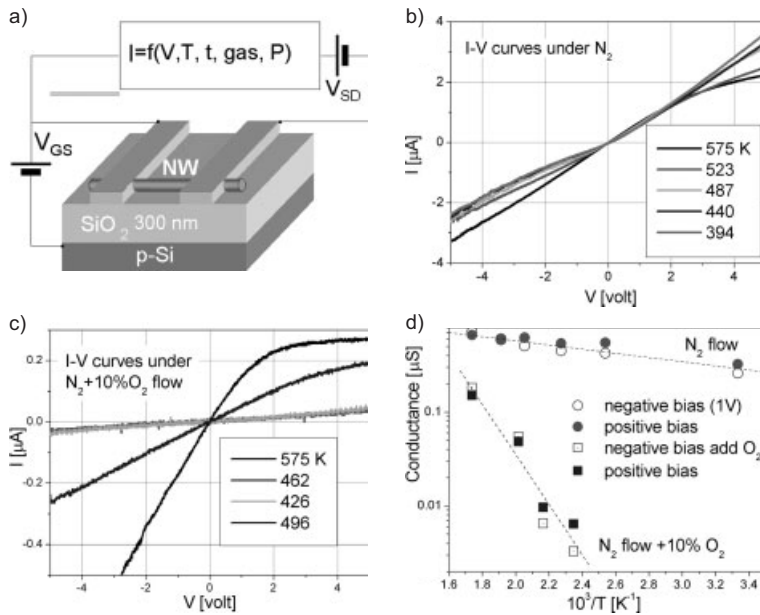


Fig. 2. Gas sensing tests on individual nanowires were carried out as a function of temperature and (flowing) ambient gas composition in a 50 mL stainless steel gas cell designed for in-situ high pressure and temperature impedance measurements. a) SnO₂ nanowires were deposited on SiO₂/Si, outfitted with vapor-deposited Au/Ti electrodes which were contacted by microscope-guided, micropositioned contacting probes. *I*-*V* characteristics for the nanowire measured in b) an inert, and c) an oxidizing environment. Nanowires were preconditioned for 2 h at 525 K under flowing dry N₂ before each set of measurements. The results shown were collected by first raising the nanowires to the highest temperature indicated, then decreasing the temperature incrementally and allowing thermal equilibrium to be established before the conductance was measured. d) The log of conductance versus inverse temperature for an individual SnO₂ nanowire in dry N₂ and N₂ + 10% O₂ atmospheres. Activation energies of 46 meV and 560 meV, respectively, are determined from the slopes, the latter indicating that, in its non-conducting state, essentially all of the shallow donor states have been depleted following oxygen chemisorption.

Exposure to oxygen (Fig. 2c) recreates the surface acceptor states (i.e., runs reactions 1 and 2 backwards) thereby reducing the nanowire's conductance and restores the temperature dependence of the conductance to the exponential form typical of intrinsic semiconductors. Combustible gases (e.g., CO) react with pre-adsorbed oxygen species like O_(s)⁻ or O_(s)²⁻ to form carbon monoxide:



reducing the steady-state surface oxygen concentration and donating a few electrons back into the bulk resulting in an increased conductivity, which depends monotonically on the gas phase partial pressure of CO. These reactions underlie the sensing mechanism towards oxidizing and reducing gases of the individual SnO₂ nanowires.

The electron exchange between the surface states and the bulk takes place within a surface layer whose thickness is of the order of the Debye length, λ_D. The key feature here is that nanowires have radius of the order of, or less than λ_D which for (bulk) SnO₂ is ~43 nm at 500 K.^[30] This means that the conductance switch alluded to above results from the operation of the nanowire alternatively as a non-conductive element in air (Fig. 3a) when the nanowire is depleted of its conduction electrons almost all of which are captured by surface acceptors, and a series of conductive states (Fig. 3a, bottom) when its surface is exposed to traces of combustible gases. This is illustrated in Figure 3b, which shows the nanowire's performance to be fully consistent with this mechanism.

The operation of the nanowire sensor conforms with previously reported empirical descriptions of sensor operation^[4] that predicts that under flat band conditions, which apply here because the nanowire's radius is ~λ_D, the electron density increase depends on CO partial pressure as Δ*n* ~ *P*_{CO}^α where the value of the exponent, α, differs somewhat according to the nature of the acceptor center.^[30] Our measurements obey this

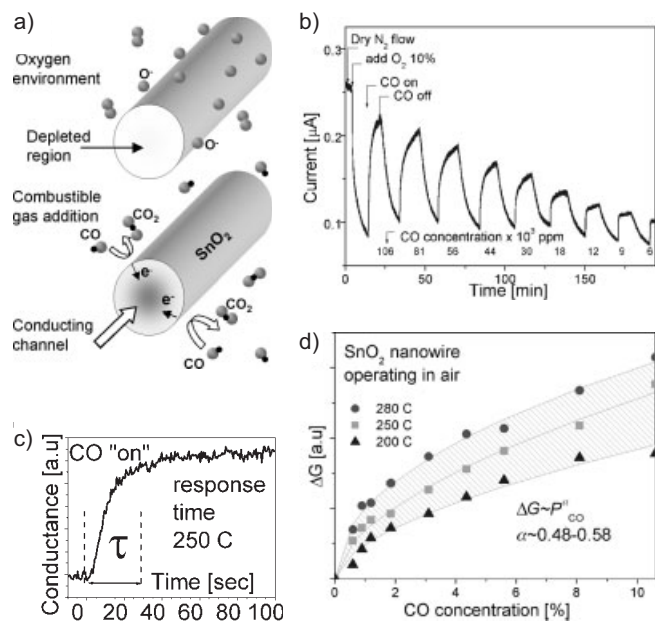


Fig. 3. The sensing mechanism of a SnO₂ nanowire involves: a) a completely depleted, hence non-conductive state under an oxidizing ambient and sharply increased conductance due to electron transfer from a surface states back into the nanowire's interior when a reducing gas (CO) is admitted. b) The response of the nanowire toward O₂ and CO pulses. The CO concentration in the flowing gas was reduced from pulse to pulse. Before the experiment was begun the nanowire was preconditioned in a constant N₂ flow. The operating voltage was 1 V, thus the ordinate corresponds to conductance in μS. c) The conductance response time of the nanowire towards 0.6% CO pulse introduced into a background N₂ + 10% O₂ mixture. d) The change in conductance of individual SnO₂ nanowires as a function of CO concentration at three values of the temperature. The data was fit to Δ*G* ∝ *P*_{CO}^α. The solid lines represent the best fit with exponent values ranging between 0.48 and 0.58.

expression well with values of α ~ 0.5 over a wide range of CO concentrations (Fig. 3d) and the temperature range used, consistent with the surface species being primarily ionosorbed oxygen (O_(s)⁻).

Immediately deducible from the above is a mode of manufacture of large nanowire arrays encompassing potentially millions of nanowires operating as highly functionalized multi-sensor arrays which can be integrated with planar technologies to create a parallel sensing device mimicking such complex functions as olfaction.

Received: January 31, 2003
Final version: February 19, 2003

Synthesis of Gallium-Filled Gallium Oxide–Zinc Oxide Composite Coaxial Nanotubes**

By Junqing Hu,* Yoshio Bando, and Zongwen Liu

One-dimensional (1D) nanoscale materials have stimulated great interest in recent years because of their unique electronic, optical, and mechanical properties and their potential technological applications in many different areas such as catalysis, magnetic recording, high-performance ceramics, and microelectronic components.^[1] After the successful synthesis of various nanotubes and nanowires, there has been great interest in the realization of layered composite nanostructures. If a multilayer structure comprising semiconducting, insulating, or metallic materials in the radial direction can be achieved in the 1D nanostructure, the utility of these materials may be further enhanced by combining uniform electronic properties in the axial direction.^[2] Thus far, different forms of multilayer nanostructures including coaxial nanocables and coaxial nanotubes have been produced by various methods. Zhang et al.^[3] have synthesized coaxial nanocables consisting of a silicon carbide core, an amorphous silicon dioxide layer, and an outer sheath of carbon and boron nitride using reactive laser ablation. Shi et al.^[4] have obtained similar nanocables with a silicon core, silicon dioxide interlayer, and carbon outer shell by combining laser ablation and thermal evaporation. Suenaga et al.^[5] have also prepared a three-layer coaxial nanocable with carbon core, boron nitride interlayer, and carbon sheath by an arc discharge method. Recently, by using carbon nanotubes as templates, various filling techniques, such as chemical insertion, physical insertion, arc encapsulation, and encapsulation via catalytic growth from the solid phase, have been employed to encapsulate foreign materials inside the carbon nanotubes for fabrication of many kinds of nanocomposite structures, and many elements and compounds have been successfully encapsulated in this confined configuration.^[6] Binary semiconducting oxide ZnO and Ga₂O₃ have distinctive properties and are widely used as transparent conducting oxide materials and optical devices and gas sensors.^[7] Now it is essential to develop a feasible method to fabricate oxide composite coaxial nanotubes, which are expected to open up new applications in the optical and sensor industries. In this communication, we sought to prepare composite Ga₂O₃–ZnO coaxial nanotubes via a simple process combining thermal reaction and physical evaporation. The as-synthesized nanotubes were either empty or partially or completely filled with Ga forming Ga (core)–Ga₂O₃ (interlayer)–ZnO (outer shell) three-layer coaxial nanocables.

- [1] N. Yamazoe, *Sens. Actuators B* **1991**, 5, 7.
- [2] W. Göpel, in *Sensors: A Comprehensive Survey* (Eds: W. Göpel, J. Hesse, J. N. Zemel), Vol. 8, VCH, Weinheim, Germany **1995**.
- [3] G. Sberveglieri, *Sens. Actuators B* **1995**, 23, 103.
- [4] J. W. Gardner, P. N. Bartlett, *Sens. Actuators B* **1994**, 18, 211.
- [5] C. Hagleitner, A. Hierlemann, D. Lange, A. Kummer, N. Kerness, O. Brand, H. Baltes, *Nature* **2001**, 414, 293.
- [6] M. C. Wheeler, J. E. Tiffany, R. M. Walton, R. E. Cavicchi, S. Semancik, *Sens. Actuators B* **2001**, 77, 167.
- [7] Y. Cui, Q. Q. Wei, H. K. Park, C. M. Lieber, *Science* **2001**, 293, 1289.
- [8] F. Favier, E. C. Walter, M. P. Zach, T. Benter, R. M. Penner, *Science* **2001**, 293, 2227.
- [9] E. Comini, G. Faglia, G. Sberveglieri, Z. Pan, Z. L. Wang, *Appl. Phys. Lett.* **2002**, 81, 1869.
- [10] J. Kong, C. W. Zhou, M. G. Chapline, S. Peng, K. J. Cho, H. J. Dai, *Science* **2000**, 287, 622.
- [11] P. G. Collins, K. Bradley, M. Ishigami, A. Zettl, *Science* **2000**, 287, 1801.
- [12] J. R. Wood, Q. Zhao, M. D. Frogley, E. R. Meurs, A. D. Prins, T. Peijs, D. J. Dunstan, H. D. Wagner, *Phys. Rev. B* **2000**, 62, 7571.
- [13] J. Kong, M. G. Chapline, H. Dai, *Adv. Mater.* **2001**, 13, 1384.
- [14] Z. W. Pan, Z. R. Dai, Z. L. Wang, *Science* **2001**, 291, 1947.
- [15] A. Michailowski, D. AlMawlawi, G. Cheng, M. Moskovits, *Chem. Phys. Lett.* **2001**, 349, 1.
- [16] Y. Huang, X. F. Duan, Q. Q. Wei, C. M. Lieber, *Science* **2001**, 291, 630.
- [17] H. J. Dai, *Surf. Sci.* **2002**, 500, 218.
- [18] C. R. Martin, *Chem. Mater.* **1996**, 8, 1739.
- [19] S. R. Nicewarner-Pena, R. G. Freeman, B. D. Reiss, L. He, D. J. Pena, I. D. Walton, R. Cromer, C. D. Keating, M. J. Natan, *Science* **2001**, 294, 137.
- [20] K. B. Shelimov, D. N. Davydov, M. Moskovits, *Appl. Phys. Lett.* **2000**, 77, 1722.
- [21] K. B. Shelimov, M. Moskovits, *Chem. Mater.* **2000**, 12, 250.
- [22] J. K. N. Mbindyo, T. E. Mallouk, J. B. Mattzela, I. Kratochvilova, B. Razaavi, T. N. Jackson, T. S. Mayer, *J. Am. Chem. Soc.* **2002**, 124, 4020.
- [23] We have just become aware of closely related work that has recently appeared: M. S. Arnold, P. Avouris, Z. W. Pan, Z. L. Wang, *J. Phys. Chem. B* **2003**, 107, 659.
- [24] H. Masuda, K. Fukuda, *Science* **1995**, 268, 1466.
- [25] D. AlMawlawi, C. Z. Liu, M. Moskovits, *J. Mater. Res.* **1994**, 9, 1014.
- [26] K. Nielsch, F. Müller, A.-P. Li, U. Gösele, *Adv. Mater.* **2000**, 12, 582.
- [27] M. Sun, G. Zangari, M. Shamsuzzoha, R. M. Metzger, *Appl. Phys. Lett.* **2001**, 78, 2964.
- [28] D. A. Popescu, J. M. Herrmann, A. Ensuque, F. Bozon-Verduraz, *Phys. Chem. Chem. Phys.* **2001**, 3, 2522.
- [29] J. H. Ding, T. J. McAvoy, R. E. Cavicchi, S. Semancik, *Sens. Actuators B* **2001**, 77, 597.
- [30] N. Barsan, U. Weimar, *J. Electroceram.* **2001**, 7, 143.

[*] Dr. J. Q. Hu, Dr. Y. Bando, Dr. Z. W. Liu
Advanced Materials Laboratory and Nanomaterials Laboratory
National Institute for Materials Science (NIMS)
Namiki 1-1, Tsukuba, Ibaraki 305-0044 (Japan)
E-mail: Hu.Junqing@nims.go.jp

[**] This work was supported by the Japan Society for the Promotion of Science (JSPS) Fellowship at the National Institute for Materials Science, Tsukuba, Japan.